

1 GROUPS OF ENCASED STONE COLUMNS: INFLUENCE OF
2 COLUMN LENGTH AND ARRANGEMENT

3
4
5
6
7
8
9
10
11
12
13
14
15
16
17
18
19
20
21
22
23

by

Jorge Castro

Group of Geotechnical Engineering

Department of Ground Engineering and Materials Science

University of Cantabria

Avda. de Los Castros, s/n

39005 Santander, Spain

Tel.: +34 942 201813

Fax: +34 942 201821

e-mail: castrogj@unican.es

Date: November 2016

Number of words: 6,000

Number of tables: 9

Number of figures: 17

The author hereby confirms that: (i) he work submitted has not been published previously,
(ii) is not under consideration for publication elsewhere, (iii) its publication is approved by
the author, and (iv) if accepted, it will not be published elsewhere, in English or in any other
language, without the written consent of the Publisher.

24 **ABSTRACT**

25 This paper presents a set of systematic 2D and 3D finite element analyses that study the
26 performance of groups of encased stone columns beneath a rigid footing. Those
27 numerical analyses show that, if the area replacement ratio, i.e. area of the columns over
28 area of the footing, and the ratio of encasement stiffness to column diameter are kept
29 constant, the column arrangement (both number of columns and column position) has a
30 small influence on the settlement reduction achieved with the treatment. For high
31 encasement stiffnesses, placing the column near the footing edges may be slightly more
32 beneficial reducing the settlement; on the contrary, the maximum hoop force at the
33 encasement is notably higher. Based on the minor influence of column arrangement,
34 this paper proposes a new simplified approach to study groups of encased stone
35 columns, which involves converting all the columns of the group beneath the footing in
36 just one central column with an equivalent area and encasement stiffness. This
37 simplified model is used to conclude that, for settlement reduction and fully encased
38 columns in a homogeneous soil, there is a column critical length of around two or three
39 times the footing width. The critical length of the encasement for partially encased
40 columns is slightly lower than that of the fully encased columns.

41

42 **KEYWORDS:** Geosynthetics, encased stone columns, numerical analyses, settlement, footings,
43 critical length.

44

45

46 **NOTATION**

47

48 a_r Area replacement ratio: $a_r = A_c/A_l$

49 c Cohesion

50 c_u Undrained shear strength

51 d_c Column diameter

52 K_0 Coefficient of lateral earth pressure at rest

53 p_a Uniform applied vertical pressure

54 p'_0 Initial mean effective stress

55 r Radius

56 s Centre-to-centre column spacing

57 s_x, s_y Horizontal displacement

58 s_z Settlement

59 s_{z0} Settlement without columns

60 x, y, z Cartesian coordinates

61

62 A Cross-sectional area

63 B Footing width

64 E Young's modulus

65 E_{oed} Oedometric (confined) modulus

66 F_g Tensile hoop force at the encasement

67 H Soft soil layer thickness

68 J_g Encasement stiffness

69 L Length

70 N Number of columns in the group

71

72 β Settlement reduction factor: $\beta = s_z/s_{z0}$

73 γ' Effective unit weight

74 ε Strain

75 ν Poisson's ratio

76 σ Stress

77 ϕ Friction angle

78 ψ Dilatancy angle

79

80 Subscripts:

81 c,s,g,l column, soil, encasement, loaded area

82 x,y,z Cartesian coordinates

83

84 **1. INTRODUCTION**

85 Ground improvement using stone columns is a popular technique for foundation of
86 embankments or structures on soft soils. Stone columns are vertical boreholes in the
87 ground, filled upwards with gravel compacted by means of a vibrator. The inclusion of
88 gravel, which has a higher strength, stiffness and permeability than the natural soft soil,
89 improves the bearing capacity of the soft foundation thus enhancing stability of the
90 embankments, reduces total and differential settlements, accelerates soil consolidation
91 and reduces the liquefaction potential (e.g. Barksdale and Bachus, 1983).

92

93 Stone columns may not be appropriate in very soft soils that do not provide enough
94 lateral confinement to the columns. In those cases, a proper shape of the column cannot
95 be ensured during installation and excessive deformation is expected upon loading. An
96 undrained shear strength of the soft soil of around 5-15 kPa (Wehr, 2006) is generally
97 adopted as the limit value to define stone column feasibility. To increase the lateral
98 confinement of the columns, and consequently, their vertical capacity, encasing the
99 columns with geotextiles or other geosynthetics has been a successful solution in recent
100 years (Alexiew and Raithel, 2015). Using horizontal geosynthetic disks placed in
101 regular vertical intervals through the column length has also shown to be an efficient
102 alternative (e.g. Ali et al., 2012 and 2014; Hosseinpour et al., 2014; Sharma et al.,
103 2004).

104

105 Stone columns and encased stone columns (ESC) are typically employed under
106 embankments or large uniformly loaded areas (e.g. Almeida et al., 2015; Chen et al.,

107 2015; Fattah et al., 2016; Yoo, 2016). In those cases, columns are distributed in a large
108 regular mesh and the problem is usually simplified to a "unit cell", i.e. only one granular
109 column, its encasement, if present, and the corresponding surrounding soil. The large
110 number of columns justifies symmetry boundary conditions. So, the lateral boundary of
111 the "unit cell" is rigid, frictionless and shear free. The simplicity of the model allows for
112 analytical solutions that provide the settlement reduction (e.g. Priebe, 1995; Raithel and
113 Kempfert, 2000; Pulko et al., 2011; Castro and Sagasetta, 2013).

114

115 More recently, stone columns have also been deployed beneath small isolated pad or
116 strip footings at low or moderate loading conditions (e.g. Watts et al., 2000). Several
117 authors (e.g. Wood et al., 2000; Castro, 2014) have studied the bearing capacity and
118 deformations of these groups of stone columns. The columns under pad or strip footings
119 may also be encased, if necessary, forming groups of ESC. However, there is little
120 information about the performance of these groups of ESC (Murugesan and Rajagopal,
121 2010; Raithel et al., 2011; Keykhosropur et al., 2012) as most studies focus on the
122 behaviour of single ESC (e.g. Malarvizhi and Ilamparuthi, 2007) or very large groups,
123 analysing only a "unit cell" (e.g. Lo et al., 2010). To the best of the author's knowledge,
124 there is no published research on the influence of the arrangement of ESC, i.e. number
125 of columns and column position, beneath a rigid footing. Besides, many papers use the
126 column length to diameter ratio, for example, to give the critical column and
127 encasements lengths (e.g. Malarvizhi and Ilamparuthi, 2007; Ali et al., 2012). This
128 paper shows that the column length to diameter ratio has a minor effect and, for
129 example, the critical column and encasement lengths should be given as a function of
130 the footing diameter or width, which is the parameter that mainly controls the

131 deformation mode.

132

133 To evaluate the performance of groups of ESC beneath rigid footings (circular or
134 square), a set of systematic 2D and 3D finite element analyses have been carried out.

135 These numerical simulations aim to show that, if the total column cross-sectional area
136 and the ratio between encasement stiffness and column radius are kept constant, the

137 column arrangement, i.e. column position and number of columns, has a minor
138 influence on the settlement reduction. That allows for a simplified two-dimensional

139 model in axial symmetry of groups of ESC beneath a rigid footing. Besides, the critical
140 column and encasement lengths are analysed. So, the paper presents firstly a

141 dimensional analysis in Section 2 to identify the main variables of the problem and the
142 corresponding dimensionless parameters. Next, the numerical models are presented

143 (Section 3). A common case is used as a reference, and using that case as a basis,
144 parametric studies are performed. The results are discussed in Section 4, showing, for

145 example, the small influence of column position within the group. That is confirmed by
146 a reanalysis of previous experimental data in Section 5 and some summarizing

147 comments on column arrangement are presented in Section 6. Using the presented
148 numerical models, the critical column and encasement lengths are evaluated in Section

149 7. Finally, some conclusions are derived.

150

151 **2. DIMENSIONAL ANALYSIS**

152 Firstly, the variables of the problem are identified and a dimensional analysis is
153 performed to get them in a dimensionless form. This dimensional analysis simplifies the

154 parametric study and helps extrapolating the results of the numerical analyses presented
155 in this paper. The variables of the problem may be classified as follows:

156 (a) Geometrical variables: Footing width, B ; soft soil layer thickness, H ; column
157 length, L_c ; encasement length, L_g ; column radius, r_c ; centre-to-centre column
158 spacing, s ; number of columns beneath the footing, N , and column position.

159 (b) Initial stress state (e.g., p'_0 , K_0) and applied vertical pressure on the footing, p_a .

160 (c) Soil, column and encasement properties: stiffness and strength.

161 (d) Results, e.g., settlement, s_z .

162

163 As the encasement thickness is usually negligible, its radius corresponds to that of the
164 column, r_c . The encasement length, L_g , may be normalised by that of the column, L_g/L_c ,
165 but this paper will show that, for groups of columns, L_g/B is more meaningful. The other
166 geometrical variables are the same as those of groups of non-encased stone columns.
167 They have been analysed in detail in Castro (2014) and only five of them are
168 independent. The following dimensionless variables are used here: H/B , L_c/B , a_r , N and
169 the column position. a_r is the area replacement ratio, which is a crucial dimensionless
170 parameter that provides the percentage of soft soil replaced by gravel, i.e. a_r is the area
171 of the columns, A_c , divided by the loaded area, A_l . Here, all the columns will be
172 assumed to be beneath the footing because it is generally more efficient (Wehr, 2004).
173 Additional columns beyond the footing increase the bearing capacity but do not
174 noticeably reduce the footing settlement (e.g. Wood et al., 2000; Castro, 2014). It is
175 worth noting that the footing width (B) or diameter plays an important role and some
176 authors (e.g. Hong et al., 2016) seem to overlook its influence. On the contrary, L_c/d_c is

177 commonly used (e.g. Dash and Bora, 2013) but it will be shown here that its influence is
178 negligible.

179

180 The soil properties depend on the constitutive model but they are either dimensionless
181 or have units of pressure. The latter ones are typically normalised using the initial stress
182 state (e.g. c_u/p'_{o}). The applied vertical pressure may be normalised using either the
183 initial stress state or a soil property (e.g. p_a/c_u). The column properties that have units
184 are usually normalised by the soil corresponding ones (e.g. the stiffness modular ratio
185 E_c/E_s).

186

187 The encasement is usually assumed to behave as a linear elastic material because its
188 strength is typically high enough. A theoretical analysis of the encasement behaviour
189 (e.g. Pulko et al., 2011) shows that the influence of the encasement stiffness, J_g , is given
190 by the following dimensionless parameter $J_g/(r_c E_{oed,s})$, where $E_{oed,s}$ is the oedometric
191 (confined) stiffness of the surrounding soil. That is valid for an elastic behaviour of the
192 surrounding soft soil; if significant plastic strains develop in the surrounding soil, it is
193 more appropriate to use a strength parameter, e.g. c_u , instead of the soil stiffness.

194

195 Finally, the settlement for a given applied pressure, p_a , is commonly related to the
196 settlement without columns, i.e. the settlement reduction factor, $\beta = s_z/s_{z0}$, to highlight
197 the improvement achieved with the column treatment.

198

199 3. NUMERICAL MODELS

200 Numerical simulations were performed to provide a better understanding of the
201 performance of ESC beneath rigid footings (circular and square). The footing settlement
202 and the stresses on soil, column and encasement were analysed. The study started with a
203 simple reference case and parametric studies were performed. In a previous publication
204 (Castro, 2014), the author showed that for non-encased stone columns, the number of
205 columns has a negligible influence, if a_r is kept constant. Here, the same will be shown
206 for ESC, if a_r and J_g/r_c are kept constant. The influence of the column and encasement
207 length will be also investigated.

208

209 3.1 Numerical code and basic assumptions

210 The finite element codes Plaxis 3D 2013 (Brinkgreve et al., 2013) and Plaxis 2D 2015
211 (Brinkgreve et al., 2015) were used for the full 3D models and the simplified 2D
212 axisymmetric models, respectively. The soft soil and the stone columns were modelled
213 as continuum elements using 10-node tetrahedral elements for the 3D cases and 15-node
214 triangular elements for 2D. The geosynthetic encasement was modelled as elements that
215 have only normal stiffness, i.e. they only have translational degrees of freedom at their
216 nodes, and can only sustain tensile stresses. In 2D, a 5-node line element was used,
217 whereas a 6-node triangular surface element was used in 3D. Perfect bonding between
218 soil, columns and their encasements at their interfaces was modelled, as it is common
219 practice (e.g. Keykhosropur et al., 2012), because they are tightly interlocked. The rigid
220 footing was assumed as perfectly rough and modelled as a very stiff plate that produces
221 uniform settlements. The finite elements for the footing were 6-node triangular elements

222 in 3D and 5-node line elements in 2D. Those elements have translational and rotational
223 degrees of freedom and their properties are the flexural rigidity and the normal stiffness.

224

225 All the numerical simulations were performed using a small strain formulation and a
226 staged construction process was modelled. Initially, the natural soft soil was modelled
227 with a horizontal ground surface and a constant thickness. Geostatic initial stresses were
228 generated using the soil unit weight and the coefficient of lateral earth pressure at rest,
229 K_0 . Later, the footing and the columns with their corresponding encasements were
230 “wished-in-place”, ignoring the changes in the natural soil due to column construction
231 (Castro and Karstunen, 2010). Finally, the loading on the footing was simulated.
232 Drained conditions were assumed for all the process, i.e. no excess pore pressures were
233 generated. Consequently, the response was studied in effective stresses. That is because
234 this paper does not focus on the stability but on the long-term settlement, as soft soils
235 can undergo large settlements at relatively low loads and the serviceability limit state
236 may be critical for the design (e.g., Black et al. 2011, McCabe and Killeen, 2016).

237

238 **3.2 Reference case**

239 The reference case consists of only one ESC under the centre of a square rigid footing.
240 The footing width, B , is 5 m and the column diameter ($d_c=1.78$ m) was chosen to give
241 an area replacement ratio of $a_r=10\%$. The value of $a_r=10\%$ may be low for a small
242 footing but it has been chosen to have a broad range of variation of column spacing and
243 number of columns for the parametric analyses. The column diameter is also high, but it
244 was chosen to have more realistic column diameters when using more realistic number

245 of columns beneath the footing (see Table 1). The column is considered to reach a rigid
246 substratum at 10 m depth. So, the column is end-bearing ($L_c/H=1$) and has a length of
247 $L_c=10$ m. The encasement was assumed to cover the full length of the column
248 ($L_g=L_c=L$). To take advantage of the symmetry of the problem, only a quarter is
249 modelled (Figure 1). The symmetry would allow for further reduction, but that is not
250 useful in this particular numerical code. Sensitivity analyses were performed to study
251 the model dimensions and a ratio of model to footing breadth of 6 was considered
252 enough. The bottom boundary is fixed and roller vertical conditions are assumed for the
253 lateral boundaries.

254

255 It is worth noting that this reference case is not equivalent to the isolated stone column
256 that is considered in many studies (e.g. Murugesan and Rajagopal, 2006) because in
257 those cases the load is applied only on top of the column, which means an $a_r=100\%$ and,
258 it is generally less efficient at reducing the settlement, yet it is useful for field load tests.

259

260 Common soil, column and encasement properties (Table 2) were used for the idealised
261 case analysed in this paper (e.g. Barksdale and Bachus, 1983; Alexiew and Raithel,
262 2015). The soil profile was simplified to only one homogeneous soil layer. An elastic-
263 perfectly plastic behaviour was considered for the soil and column using the Mohr-
264 Coulomb yield criterion and a non-associated flow rule, with a constant dilatancy angle.
265 A Poisson's ratio of $\nu_s=\nu_c=0.33$ was assumed for the soil and column and their Young's
266 moduli were taken as $E_s=2$ MPa and $E_c=30$ MPa, respectively. That means a modular
267 ratio of 15. Although the crushed stone (gravel) used for the column backfill is a pure
268 frictional material, a small cohesion ($c_c=0.1$ kPa) was used to avoid numerical problems.

269 Typical values of $\phi_c=40^\circ$ and $\psi_c =5^\circ$ were chosen for the gravel. For the soft soil,
270 representative cohesion and friction angle ($c_s=3$ kPa and $\phi_s=23^\circ$) were assumed within
271 the common range. The soil was considered as a non-dilatant material. A stiffness of
272 $J_g=2000$ kN/m was taken for the geosynthetic encasement and a null Poisson's ratio
273 ($\nu_g=0$) because the geosynthetic encasement was assumed to have two major directions
274 (radial and longitudinal), which behave independently (e.g. Soderman and Giroud,
275 1995; Castro, 2016).

276

277 A uniform vertical pressure of $p_a=100$ kPa was applied on the rigid footing. This
278 applied pressure is high enough to produce significant plastic strains. For the sake of
279 simplicity, the ground water level was assumed to be at the ground surface and an
280 effective unit weight of $\gamma'=10$ kN/m³ for soil and column was directly considered
281 without modelling pore water pressures. The coefficient of lateral earth pressure at rest
282 was set equal to $K_0=0.6$, using the Jaky's formula for the soil and disregarding
283 installation effects.

284

285 **3.3 Parametric studies**

286 Using the reference case as a starting point, parametric studies were carried out varying
287 several properties:

288 (a) Column arrangement. The number of columns, N , the centre-to-centre column
289 spacing, s , and their positions were varied. Typical column configurations were used.
290 For the sake of comparison, the number of columns was varied without changing the
291 area replacement ratio, a_r , and consequently, the diameter of the columns is obtained

292 using a_r , N and B . The J_g/d_c ratio was also kept constant. So, depending on the number
293 of columns, the encasement stiffness was varied to get the same J_g/d_c ratio as in the
294 reference case.

295

296 (b) Other geometric factors. The size of the footing B , the length of the encasement and
297 columns L_g , L_c , the soft soil layer thickness H and the area replacement ratio, a_r .

298 (c) Material properties. In the previous parametric studies, the normalised encasement
299 stiffness was varied from a null value, i.e. no encasement, to a high enough value.
300 Besides, a specific parametric study of the strength of the soil was also performed.
301 Other column or soil parameters, such as their stiffnesses, were not varied because of
302 their less important effect.

303

304 **3.4 Mesh sensitivity analyses**

305 Some mesh dependency was foreseen due to the problem configuration, i.e. a rigid
306 footing in a 3D mesh. A preliminary analysis of several column groups confirmed a
307 slight mesh dependency. Due to computational restrictions, the number of elements is
308 limited in the 3D mesh. Therefore, for the mesh sensitivity analyses, the square footing
309 was changed to a circular one with the same area to have axial-symmetry and model the
310 problem also in a fine enough 2D mesh (Figure 2). In fact, the main improvement in the
311 2D simulations is not caused by the number of elements but by their higher order (i.e.
312 15-node triangular elements in 2D and 10-node tetrahedral elements in 3D for soil and
313 column elements).

314

315 The results of the mesh sensitivity analyses are summarized in Figure 3, where the
316 settlement simulated using the 3D mesh is compared with that using the fine enough 2D
317 mesh. For each number of elements, the most accurate mesh was also searched, i.e.
318 refining the mesh in the area of interest (footing, column and encasement) and using a
319 coarse mesh in the far field (Figure 1). For all the parametric studies, it was decided to
320 use comparable meshes of around 65-75 thousand elements with the same degree of
321 relative refinement. Although those meshes slightly underpredict the settlement (around
322 5%), they are perfectly valid to compare and identify trends in the parametric studies.

323

324 **4. RESULTS AND DISCUSSION**

325 **4.1 Column position**

326 The first parametric study focused on the influence of column spacing, or more
327 precisely, the relative position of the columns beneath the footing. A group of four stone
328 columns ($N=4$) was used, keeping constant the area replacement ratio of the reference
329 case ($a_r=10\%$) and the J_g/d_c ratio; so, $d_c=0.89$ m and $J_g=1000$ kN/m. The spacing
330 between columns was varied from $s=1$ to 4 m (Figure 4). Besides, two additional
331 encasement stiffnesses were studied, namely no encasement ($J_g=0$) and $J_g=2500$ kN/m.
332 The settlements of the groups of non-encased and encased columns ($N=4$) were
333 compared with the settlements of the cases with a single column ($N=1$) and similar
334 results were found (Figure 5). On one hand, the settlement is slightly higher when the
335 columns are close to the edges of the footing for the non-encased columns and on the
336 other hand, the settlement is lower for the encased columns when the columns are close
337 to the footing edges. The two main effects that control the influence of the column

338 position on the settlement reduction are:

- 339 – when the columns are close to the edges, they tend to support higher vertical
340 stresses because the stresses are higher at the edges for a rigid footing;
- 341 – when the columns are close to the centre, the surrounding vertical and horizontal
342 stresses are higher and, therefore, the columns are better laterally confined.

343

344 Both effects mostly balance each other out, but depending on the soil, column and
345 encasement properties one may be slightly more beneficial than the other (Figure 5). For
346 the encased columns, if they are close to the edges ($s=4$ m), they support higher vertical
347 stresses than those close to the centre ($s=1$ m) (Figure 6). For the non-encased columns
348 ($J_g=0$), the positive effect of positioning the columns close to the edges disappears
349 because their lateral support is lower and their lateral expansions cause a slight increase
350 in the settlement (Figure 5).

351

352 Column position has a small influence on the settlement of groups of encased columns.
353 However, the maximum circumferential or hoop tensile force of the encasement (F_g)
354 notably increases when the columns are close to the footing edges (Figure 7), e.g. from
355 14.5 to 22.8 kN/m for column spacings of $s=1$ and 4 m, respectively. As previously
356 mentioned, the vertical stresses are higher near the edges of a rigid footing and that
357 cause a higher maximum of the tensile encasement force F_g , when the columns are close
358 to the footing edges. Figure 7 shows the circumferential tensile force of the encasement
359 for a diagonal cross section and at the outer boundary. Although the tensile force F_g is
360 slightly higher at the outer boundary than at the inner boundary, F_g is quite similar all
361 around the encasement for the same depth. The fact that a greater maximum F_g

362 develops, when the columns are close to the footing edges, could lead to think that in
363 those cases the encasement contribution is more important and then, the settlement is
364 further reduced. However, that is not the case, since the average F_g of the encasement is
365 similar for different spacings (Figure 7).

366

367 The depth of maximum F_g depends of the column mode of deformation, and this, in
368 turn, depends on the encased column position. So, in this case, for a column spacing of
369 $s=1$ m, the maximum F_g is located at 3 m depth, i.e. $z/B=0.6$, because bulging is the
370 main mode of deformation for centre columns. On the other hand, for columns close to
371 the footing edges, shearing is the main mode of deformation, and the maximum F_g
372 occurs at shallow depths, e.g. at 0.7 m depth for $s=4$ m. The zones of maximum
373 shearing and bulging within the columns are directly related to the deformation beneath
374 a rigid footing (Figure 8 and Figure 9).

375

376 **4.2 Number of columns**

377 The next parametric study focused on the influence of the number of columns, which
378 was varied between $N=1$ and 24 in multiples of 4 to retain the symmetry. The variation
379 of the number of columns inevitably leads to some changes in the column position. To
380 reduce that influence, all the columns were uniformly placed along a square with a side
381 length of 4 m. Besides, two different column configurations were used, one with a
382 column at the corner of the square and another with columns just on the sides (Figure
383 10). The diameter of the columns (d_c) and the encasement stiffness (J_g) were varied
384 accordingly to keep a_r and J_g/d_c constant (Table 1).

385

386 The results show the small influence of the number of columns on the settlement
387 reduction (Table 3). There are some differences but they may be attributed mainly to the
388 differences in the column position because they follow the same trends as those in the
389 previous section. It is worth noting that for each number of columns, the ratio L/d_c is
390 different (from roughly 5 up to 27) because $a_r=10\%$ is kept constant. That demonstrates
391 the minor influence of the L/d_c ratio on the settlement reduction for a constant
392 normalised encasement stiffness (J_g/d_c). Just for very high values of the L/d_c ratio, i.e.
393 very slender columns, there may appear second order effects or low-quality finite
394 elements.

395

396 Contrary to the settlement reduction, the maximum hoop force at the encasement (F_g)
397 notably changes (Table 4). The differences are mainly caused by the varying stiffness of
398 the encasement for different number of columns (Table 1). The encasement was
399 assumed to behave as a linear elastic material; so, it may be easily demonstrated that
400 $F_g=J_g \varepsilon_r$, where ε_r is the radial strain. In this way, the hoop force may be normalised by
401 the encasement stiffness (F_g/J_g). Those normalised values are not affected by the
402 number of columns, N (Table 5). However, F_g/J_g notably varies with many other
403 factors, such as column position, normalised encasement stiffness (J_g/d_c) or surrounding
404 soil strength.

405

406 It is worth noting that the hoop force at the encasement (F_g) may oscillate due to strain
407 localization as pointed out by Pulko et al. (2011) and Castro and Sagaseta (2011).
408 Besides, the hoop force, and particularly its maximum value, is more mesh sensitive

409 than the settlement.

410 **4.3 Soil properties**

411 As already mentioned, only the strength of the soil was altered because other column
412 and soil parameters, such as their stiffnesses, have a less important effect. Small
413 differences were found in the settlement reduction between different column
414 configurations (Table 6a) except for the softest soil ($\phi_s=20^\circ$; $c_s=1$ kPa), which is not a
415 desired case because of the large zone at failure (Figure 11). The soil strength affects the
416 two commented phenomena related to column position. So, an encased column usually
417 reduces the settlement further if placed near the footing edges. This effect is more
418 pronounced if the surrounding soil is very soft. On the other hand, the hoop forces at the
419 encasement are notably higher (Table 6b).

420

421 **4.4 Soil layer thickness and footing width**

422 The soil layer thickness was varied to study its influence on the settlement reduction
423 (Table 7). For end-bearing columns ($L=H$), that is analogous to vary the footing width
424 because the ratio H/B is the governing parameter. In fact, H/B indicates the extension of
425 the load and whether it is a small footing or a large loaded area that can be studied using
426 the “unit cell” concept. When H/B decreases and the columns are not near the footing
427 edges, the lateral confinement of the columns improves. So, the slight positive effect of
428 positioning the columns near the footing edges for $H/B=2$ (reference case) vanishes for
429 $H/B=1.2$ (similar settlement for different column spacings). For values of H/B lower
430 than 1.2, positioning the columns beneath the centre of the footing gives slightly less
431 settlement (Table 7).

432

433 **4.5 Column length**

434 So far, only end-bearing columns had been modelled ($L=H$). Now, the column and
435 encasement lengths were reduced to study their influence (Figure 12). For the sake of
436 simplicity, the floating columns are assumed to be fully encased, i.e. $L=L_g=L_c$. For
437 floating columns, the column position is slightly more relevant than for end-bearing
438 columns because there is a new effect:

- 439 – Column punching or penetration into the underlying soil, which is related to the
440 deformation of the soil layer that is not improved beneath the columns.

441

442 For the same area replacement ratio, column penetration into the underlying soil is
443 greater when there is less number of columns and with closer spacings (Figure 12 and
444 Table 8). In this regard, the behaviour is similar to that of non-encased columns (Wood
445 et al., 2000; Castro, 2014), where column penetration is greatest when the columns are
446 in the middle of the footing, they are short and a_r is high. When the column tip is near
447 the vertex of the pyramid created by the maximum shear strain contours, the column
448 notably punches into the underlying soil, e.g. for a central column and L/B around 1
449 (Figure 8c and Figure 9). Therefore, columns near the edges give slightly less settlement
450 than central columns for those column lengths ($L\approx B$) (Figure 12).

451

452 The number of columns has less influence on the settlement reduction than their
453 position (Table 8). Nevertheless, an increasing number of columns reduces the column
454 punching because it distributes the load on the underlying layer; therefore, slightly less

455 settlement is computed.

456

457 In summary, when floating columns reach a critical length (for example, $L=8$ m in this
458 case), their behaviour is similar to that of end-bearing columns. If they are shorter,
459 distributing the columns beneath the footing (more columns and near the footing edges)
460 gives slightly less settlement. Yet, the differences are not very important, namely
461 smaller than 20% (Figure 12 and Table 8).

462

463 **4.6 Area replacement ratio**

464 The value of $a_r=10\%$ may be low for a small footing because it has been chosen to have
465 a broad range of variation of column spacing and number of columns. So, the study was
466 extended to higher values of a_r , namely 20% and 30%. The results (Table 9) show
467 similar trends to those obtained with $a_r=10\%$. Only two subtle differences were found:

- 468 – For end-bearing columns ($L=H=2B$), the slight beneficial effect of positioning
469 the columns near the footing edges (e.g., $s=3$ m) vanishes for higher area
470 replacement ratios (e.g., $a_r=30\%$). In the present analysis, the encasement
471 stiffness was kept constant for different area replacement ratios and then, its
472 contribution to the lateral confinement of the column is lower for higher area
473 replacement ratios.
- 474 – For floating columns ($L=B$), the punching of the columns slightly increases with
475 the area replacement ratio, as already mentioned and similarly to non-encased
476 columns (Wood et al., 2000).

477

478 **5. ANALYSIS OF PREVIOUS EXPERIMENTAL DATA**

479 It is difficult to find previous experimental data in the literature that allow to study the
480 influence of the column arrangement beneath a rigid footing. Ali et al. (2014) compare
481 the results of laboratory small-scale tests on single and groups of encased columns. The
482 advantage of this case is that the area replacement ratio beneath the footing and the
483 column diameter are roughly the same in both cases.

484

485 The analysis of those data (Figure 13) shows that the results for a single column and for
486 a group of three columns are very similar, which confirms the small influence of the
487 column arrangement beneath a rigid footing. It is worth noting that there are differences
488 between both cases: the footing diameter is 60 mm for the single column and 96 mm for
489 the group of columns and the area replacement ratio is 25% for the single column and
490 29% for the group of columns. For the group of columns, there are also extra column
491 outside the footing. However, these differences nearly compensate between each other,
492 being the settlement for the single column slightly lower due to the smaller footing
493 dimensions. For the case without encasement, the results of a single column and footing
494 diameter of 100 mm (Ali et al., 2012) are also included to show that in this case the
495 settlement is higher due to the bigger footing diameter. It is worth noting that Ali et al.
496 (2014) seem to neglect the influence of the footing width (B) and also that the effect of
497 the encasement is controlled by the parameter J_g/d_c and then, the results for the same
498 type of encasement but with different column diameter are not comparable.

499

500 **6. COMMENTS ON COLUMN ARRANGEMENT**

501 This paper shows the small influence of column arrangement in groups of ESC beneath
502 a rigid footing on the reduction of settlement achieved with a ESC treatment. Similar
503 results were found for the full 3D model and for the 2D axisymmetric model with an
504 equivalent central column that keeps both a_r and J_g/d_c (Figure 2 and Table 1). Besides,
505 the central column generally gives results on the safe side (e.g. Table 6a) and the 2D
506 mesh is less computational demanding and generally uses more elements of higher
507 order, providing more accurate results. That “one column” model may be useful not
508 only for numerical analyses but also for analytical approaches.

509

510 In practise, uniformly distributed columns beneath the footing is the usual
511 configuration. The small influence of the column arrangement on the settlement
512 reduction found in this paper justifies that construction practise, because uniformly
513 distributed columns are more beneficial for some other factors not included in this
514 study, such as bending moments in the footing, soil drainage and easiness of
515 construction.

516

517 **7. CRITICAL COLUMN AND ENCASEMENT LENGTHS**

518 The simplified model of only one column is used here to investigate the critical or
519 optimal column and encasement lengths. For non-encased stone columns, there is a
520 critical length of the columns around $1.5-2B$ for settlement reduction (Wehr, 2004;
521 Castro, 2014). It is worth noting that many authors (e.g. Malarvizhi and Ilamparuthi,

2007; Ali et al., 2012) give critical lengths as a function of the column diameter, but as it has been here shown (Table 3), the column length to diameter ratio has a minor influence by itself. For settlement reduction, the critical column length is related to the pressure bulb that the footing generates (Figure 14a), and for footing bearing capacity, the critical length depends on the failure mechanism (Figure 14b). As the critical length for settlement reduction is longer, that is usually the considered value. For large loaded areas (high values of B), the critical column length is higher than the soft layer thickness, and consequently, the concept of critical or optimal length does not apply. For encased columns, Figure 15 shows that the critical length of fully encased columns varies between $1.9-3.3B$ for the studied cases. These values are higher than for non-encased columns because the columns are better laterally confined and transmit the load deeper. For the reference case (Figure 15a, dashed lines), the rigid bottom is not far enough ($H/B=2$) to clearly identify the critical length. Therefore, the size of the footing was reduced ($H/B=4$) to better illustrate the critical length of the column (solid lines).

536

In the present case, there are important plastic strains and the critical length of the column is related to the extent of those plastic strains with depth (Figure 16). The critical length of the column is slightly lower for higher area replacement ratios (Figure 15a, solid lines) because the extent of the plastic strains decreases with a_r , i.e. $2.6B$ for $a_r=10\%$, $2.4B$ for $a_r=20\%$ and $2.3B$ for $a_r=50\%$ (Figure 16).

542

The critical length of the column depends on the problem variables, e.g. the strength of the surrounding soft soil. For a higher strength of the surrounding soft soil ($c_s=10$ kPa and $\phi_s=30^\circ$), the plastic strains are reduced and also their extent with depth.

546 Consequently, the critical column length is lower ($1.9B$), but the elastic strains below
547 the column tip are relatively more significant (Figure 15b). On the other hand, the
548 encasement stiffness also plays an important role because, for higher encasement
549 stiffnesses (e.g. $J_g=5000$ kN/m), the applied load is transferred to deeper layers, and
550 consequently, the critical column length is higher ($2.5-3.3B$ in this case, Figure 15c).

551

552 The previous analyses are for fully encased stone columns, i.e. ($L_g=L_c$) that do not
553 necessarily reach a rigid stratum ($L<H$). Some authors (e.g. Murugesan and Rajagopal,
554 2006, 2007) have proposed to partially encased the columns. Murugesan and Rajagopal
555 (2006, 2007) studied isolated columns, i.e. $B=d_c$ and $a_r=100\%$, and found a critical
556 encasement length of $L_g=2-3d_c=2-3B$. Yoo (2010) already noted that the critical
557 encasement length depends strongly on the loading type and found that for embankment
558 loading there was not a critical depth and confirmed the results of Murugesan and
559 Rajagopal (2006, 2007) for isolated column loading. Castro et al. (2013) also found
560 using analytical solutions that for embankment loading, there is not a sharp change in
561 reducing the settlement when varying the encasement length.

562

563 To analyse the critical length of the encasement, columns that reach a rigid substratum
564 ($L_c=H$) but are partially encased ($L_g<L_c$) were numerically simulated. The results
565 (Figure 17) show that there is a critical length for the encasement that varies between
566 1.4 and $2.8B$ for the analysed cases. The critical length of the encasement also depends
567 on the pressure bulb generated by the footing; so, the length of the encasement was also
568 normalised by the footing width, L_g/B . The critical length of the encasement is slightly
569 lower than that of the column because it is related to the extent of the plastic strains just

570 in the surrounding soil (Figure 16). For the reference case, those values are $1.9B$ for
571 $a_r=10\%$, $1.7B$ for $a_r=20\%$ and $1.4B$ for $a_r=50\%$. The critical length of the encasement is
572 slightly reduced for higher strengths of the surrounding soil (Figure 17b) and increases
573 for higher encasement stiffnesses (Figure 17c).

574

575 In conclusion, the critical column and encasement lengths are mainly controlled by the
576 size of the footing, B . The critical length of the columns is $1.5-2 B$ for non-encased
577 columns, these values are higher for encased columns (around $2-3.5B$, higher values for
578 higher encasement stiffnesses) because encased columns transfer the load deeper. On
579 the other hand, the critical length of the encasement is only slightly lower than that of
580 the column (around $1.5-3B$). So, in most cases where partially encasing the column is
581 effective, reducing the total column length would be more economical.

582

583 **CONCLUSIONS**

584 The paper presents a set of systematic numerical analyses of groups of encased stone
585 columns beneath a rigid footing. If the area replacement ratio (a_r) and the normalised
586 encasement stiffness (J_g/d_c) are the same, the column arrangement (both column
587 position and number of columns) has a small influence on the settlement reduction. The
588 column position is slightly more relevant than the number of columns because of the
589 following two effects:

590 1) Near the edges of a rigid footing, the vertical stresses are higher, so columns
591 near the edges would tend to support higher loads.

592 2) On the contrary, columns beneath the center are better laterally confined.

593 Both effects tend to balance each other out, but depending on the case, one may be
594 slightly more beneficial than the other.

595

596 For floating columns, there appears a third effect:

597 3) Column punching or penetration into the underlying soil.

598 This effect causes further differences between different column arrangements but
599 disappears once the column length is higher than a critical or optimal one.

600

601 The small influence of the column arrangement on the settlement reduction may allow
602 for a 2D axisymmetric model with an equivalent central column that retains both a_r and
603 J_g/d_c .

604

605 In a homogeneous soil layer, encased columns beneath a rigid footing have a critical
606 length of around $2-3.5B$ for settlement reduction. The critical length depends on the
607 extent of plastic strains, increases with the encasement stiffness and decreases with the
608 area replacement ratio and the soil strength.

609

610 The critical length of the encasement for partially encased column is slightly lower
611 (around $1.5-3B$), depends on the plastic strains in the surrounding soft soil and also
612 increases with the encasement stiffness and decreases with the area replacement ratio
613 and the soil strength.

614

615 The presented analysis is mainly based on finite element simulations; further
616 experimental investigation is necessary to confirm the above conclusions.

617

618 **REFERENCES**

- 619 Alexiew, D., Raithel, M., 2015. Geotextile-Encased Columns: Case Studies over Twenty Years,
620 in: Indraratna, Chu, Rujikiatkamjorn (Eds.), Embankments with Special Reference to
621 Consolidation and Other Physical Methods. Butterworth-Heinemann, pp. 451-477.
- 622 Ali, K., Shahu, J.T., Sharma, K.G., 2012. Model tests on geosynthetic-reinforced stone
623 columns: a comparative study. *Geosynth. Int.* 19 (4), 433-451.
- 624 Ali, K., Shahu, J.T., Sharma, K.G., 2014. Model tests on single and groups of stone columns
625 with different geosynthetic reinforcement arrangement. *Geosynth. Int.* 21 (2), 103-118.
- 626 Almeida, M., Hosseinpour, I., Riccio, M., and Alexiew, D., 2015. Behavior of Geotextile-
627 Encased Granular Columns Supporting Test Embankment on Soft Deposit. *J. Geotech.*
628 *Geoenviron. Eng.* 141(3), 04014116.
- 629 Barksdale, R.T., Bachus, R.C., 1983. Design and construction of stone columns. Report
630 FHWA/RD-83/026. Nat Tech Information Service, Springfield.
- 631 Black, J.A., Sivakumar, V., Bell, A., 2011. The settlement performance of stone column
632 foundations. *Géotechnique* 61(11), 909-922.
- 633 Brinkgreve, R.B.J., Engin, E., Swolfs, W.M., 2013. *Plaxis 3D 2013 Manual*. Plaxis bv, the
634 Netherlands.
- 635 Brinkgreve, R.B.J., Kumarswamy, S., Swolfs, W.M., 2015. *Plaxis 2D 2015 Manual*. Plaxis bv,
636 the Netherlands.
- 637 Castro, J., 2014. Numerical modelling of stone columns beneath a rigid footing. *Comput.*
638 *Geotech.* 60, 77-87.
- 639 Castro, J., 2016. Discussion of “Column Supported Embankments with Geosynthetic Encased
640 Columns: Validity of the Unit Cell Concept”. *Geotech. Geol. Eng.* 34(1), 419-420.

- 641 Castro, J., Karstunen, M., 2010. Numerical simulations of stone column installation. Can.
642 Geotech. J., 47(10), 1127-1138.
- 643 Castro, J., Sagaseta, C., 2011. Deformation and consolidation around encased stone columns.
644 Geotext. Geomembr. 29, 268-276.
- 645 Castro, J., Sagaseta, C., 2013. Influence of elastic strains during plastic deformation of encased
646 stone columns. Geotext. Geomembr. 37, 45-53.
- 647 Castro, J., Sagaseta, C., Cañizal, J., Da Costa, A., Miranda, M., 2013. Foundations of
648 embankments using encased stone columns. Proc. 18th Int. Conf. Soil Mech. Geotech.
649 Eng., Vol. 3, pp. 2445-2448. Paris, France.
- 650 Chen, J.-F., Li, L.-Y., Xue, J.-F., Feng, S.-Z., 2015. Failure mechanism of geosynthetic-encased
651 stone columns in soft soils under embankment. Geotext. Geomembr. 43(5), 424-431.
- 652 Dash, S.K., Bora, M.C., 2013. Influence of geosynthetic encasement on the performance of
653 stone columns floating in soft clay. Can. Geotech. J. 50(7), 754-765.
- 654 Fattah, M., Zabar, B., and Hassan, H., 2016. Experimental Analysis of Embankment on
655 Ordinary and Encased Stone Columns. Int. J. Geomech. 16(4), 04015102.
- 656 Hong, Y.-S., Wu, C.-S., Yu, Y.-S., 2016. Model tests on geotextile-encased granular columns
657 under 1-g and undrained conditions. Geotext. Geomembr. 44(1), 13-27.
- 658 Hosseinpour, I., Riccio, M., Almeida, M.S.S., 2014. Numerical evaluation of a granular column
659 reinforced by geosynthetics using encasement and laminated disks. Geotext. Geomembr.
660 42(4), 363-373.
- 661 Keykhosropur, L., Soroush, A., Imam, R., 2012. 3D numerical analyses of geosynthetic encased
662 stone columns. Geotext. Geomembr. 35, 61-68.
- 663 Lo, S.R., Zhang, R., Mak, J., 2010. Geosynthetic-encased stone columns in soft clay: a
664 numerical study. Geotext. Geomemb. 28 (3), 292-302.
- 665 Malarvizhi, S.N. Ilamparuthi, K., 2007. Comparative study on the behaviour of

666 encased stone column and conventional stone column. *Soils Found.* 47(5), 873–885.

667 McCabe, B.A., Killeen, M.M., 2016. Small Stone-Column Groups: Mechanisms of Deformation
668 at Serviceability Limit State. *Int. J. Geomech.* 2016; 0406114.

669 Murugesan, S., Rajagopal, K., 2006. Geosynthetic-encased stone columns: Numerical
670 evaluation. *Geotext. Geomem.* 24(6), 349–358.

671 Murugesan, S., Rajagopal, K., 2007. Model tests on geosynthetic encased stone columns.
672 *Geosynthet. Int.* 14(6), 346–354.

673 Murugesan, S. Rajagopal, K., 2010. Studies on the Behavior of Single and Group of
674 Geosynthetic Encased Stone Columns. *J. Geotech. Geoenviron. Eng.* 136(1), 129–139.

675 Priebe, H.J., 1995. Design of vibro replacement. *Ground Eng.* 28(10), 31-37.

676 Pulko, B., Majes, B., Logar, J., 2011. Geosynthetic-encased stone columns: Analytical
677 calculation model. *Geotext. Geomembr.* 29(1), 29-39.

678 Raithel, M., Kempfert, H.G., 2000. Calculation models for dam foundations with geotextile
679 coated sand columns. In: *Proceedings of the International Conference on Geotechnical &*
680 *Geological Engineering, GeoEngg—2000, Melbourne.*

681 Raithel, M., Werner, S., Küster, V., Alexiew, D., 2011. Analyse des Trag- und
682 Verformungsverhaltens einer Gruppe geokunststoffummantelter Säulen im Großversuch.
683 *Bautechnik* 88, Heft 9, 593-601.

684 Sharma, S.R., Phanikumar, B.R., Nagendra, G., 2004. Compressive load response of granular
685 piles reinforced with geogrids. *Can. Geotech. J.* 41 (1), 187–192.

686 Soderman, K.L., Giroud, J.P., 1995. Relationships between uniaxial and biaxial stresses and
687 strains in geosynthetics. *Geosynth. Int.* 2(2), 495-504.

688 Watts, K.S, Johnson, D., Wood, L.A., Saadi, A., 2000. An instrumented trial of vibro ground
689 treatment supporting strip foundations in a variable fill. *Géotechnique* 50(6), 699-708.

- 690 Wehr, J., 2004. Stone columns – single columns and group behaviour. Proc. 5th Int. Conf.
691 Ground Improvement Tech., Kuala Lumpur, pp. 329-340.
- 692 Wehr, J., 2006. The undrained cohesion of the soil as criterion for the column installation with a
693 depth vibrator. In: Proceedings of the International Symposium on vibratory pile driving
694 and deep soil vibratory compaction, TRANSVIB 2006, Paris.
- 695 Wood, D.M., Hu, W., Nash, D.F.T., 2000 Group effects in stone column foundations: model
696 tests. *Géotechnique* 50(6), 689-698.
- 697 Yoo, C., 2010. Performance of Geosynthetic-Encased Stone Columns in Embankment
698 Construction: Numerical Investigation. *J. Geotech. Geoenviron. Eng.* 136(8), 1148–1160.
- 699 Yoo, C., 2016. Settlement behavior of embankment on geosynthetic-encased stone column
700 installed soft ground – A numerical investigation. *Geotext. Geomembr.* 43(6), 484-492.
- 701
- 702

703 **TABLE CAPTIONS**

704 Table 1. Column diameter and encasement stiffness for different number of columns.

705 Table 2. Soft soil and column properties for reference case

706 Table 3. Settlement (mm) for different number of columns.

707 Table 4. Maximum hoop force at the encasement, F_g (kN/m), for different number of
708 columns.

709 Table 5. Normalised maximum hoop force at the encasement, F_g/J_g (%), for different
710 number of columns.

711 Table 6. Results for different soil material strengths. Reference case: (a) Settlement
712 (mm); (b) Maximum hoop force at the encasement (kN/m).

713 Table 7. Settlement (mm) for different soil layer thicknesses.

714 Table 8. Results for different column lengths. Reference case: (a) Settlement (mm); (b)
715 Maximum hoop force at the encasement (kN/m).

716 Table 9. Settlement (mm) for different area replacement ratios.

717

718 **FIGURE CAPTIONS**

- 719 Figure 1. 3D finite element model. Reference case.
- 720 Figure 2. 2D finite element model. Reference case. Circular footing.
- 721 Figure 3. Mesh sensitivity analyses.
- 722 Figure 4. Groups of stone columns for different column positions.
- 723 Figure 5. Influence of column position.
- 724 Figure 6. Vertical stresses beneath the footing. Diagonal section.
- 725 Figure 7. Circumferential tensile force of the encasement for different column spacings.
- 726 Figure 8. Deformation modes: (a) Bulging; (b) Shearing; (c) Punching. Deformed mesh
727 (amplified 10 times). Cross section.
- 728 Figure 9. Incremental shear strains. Blue (dark) lowest value (0) and red highest value
729 (2%). Cross section.
- 730 Figure 10. Groups of encased stone columns for different number of columns.
- 731 Figure 11. Zones at failure: (a) $\phi_s=23^\circ$ and $c_s=3$ kPa; (b) $\phi_s=20^\circ$ and $c_s=1$ kPa. Black
732 zones: relative shear stress between 99 and 100% of failure.
- 733 Figure 12. Influence of column length for different column positions.
- 734 Figure 13. Comparison between small-group and single column. Laboratory tests (Data
735 taken from Ali et al., 2014).
- 736 Figure 14. Conceptual justification of critical column length in a homogeneous soil
737 layer: (a) for settlement reduction; (b) for bearing capacity.
- 738 Figure 15. Critical column length for different area replacement ratios and encasement
739 and soil properties. 1 Column (2D) and $B=2.5$ m: (a) Reference case; (b) $c_s=3$
740 kPa and $\phi_s=30^\circ$; (c) $J_g=5000$ kN/m.
- 741 Figure 16. Plastic points (in red). Reference case. 1 Column (2D) and $B=2.5$ m: (a)
742 $a_r=10\%$; (b) $a_r=20\%$; (c) $a_r=50\%$.
- 743 Figure 17. Critical partial encasement length for different area replacement ratios and
744 encasement and soil properties. 1 Column (2D) and $B=2.5$ m: (a) Reference
745 case; (b) $c_s=3$ kPa and $\phi_s=30^\circ$; (c) $J_g=5000$ kN/m.

746

747 Table 1. Column diameter and encasement stiffness for different number of columns.

	$a_r=10\%$	$J_g/d_c=1120$ kPa	$J_g/d_c=2800$ kPa
	d_c (m)	J_g (kN/m)	J_g (kN/m)
$N=1$	1.784	2000	5000
$N=4$	0.892	1000	2500
$N=8$	0.631	707.4	1768
$N=12$	0.515	577.4	1443
$N=16$	0.446	500.0	1250
$N=20$	0.399	447.3	1118
$N=24$	0.364	408.1	1020

748

749

750

751 Table 2. Soft soil and column properties for reference case.

	γ'	K_0	c	ϕ	ψ	ν	E
	(kN/m ³)	(-)	(kPa)	(°)	(°)	(-)	(MPa)
Soft soil	10	0.6	3	23	0	0.33	2
Stone column	10	0.6	0.1	40	5	0.33	30

752

753

754 Table 3. Settlement (mm) for different number of columns.

	L/d_c	$J_g/d_c=0$		$J_g/d_c=1120$ kPa		$J_g/d_c=2800$ kPa	
		Corner	Sides	Corner	Sides	Corner	Sides
2D	5.6	237.6		192.4		164.7	
Circular	5.6	226.9		182.6		156.0	
$N=1$	5.6	229.5		184.2		156.8	
$N=4$	11.2	231.4	227.3	176.5	179.3	146.5	150.8
$N=8$	15.9	231.0	226.8	176.6	177.0	147.9	148.4
$N=12$	19.4	228.9	226.2	176.6	177.1	147.4	148.5
$N=16$	22.4	227.3	226.6	176.4	176.7	147.5	148.3
$N=20$	25.1	226.3	225.2	175.5	176.1	147.1	148.1
$N=24$	27.5	225.1	224.9	174.4	175.6	146.3	147.7

755 2D, Circular and $N=1$: central column

756

757 Table 4. Maximum hoop force at the encasement, F_g (kN/m), for different number of
758 columns.

	$J_g/d_c=1120$ kPa		$J_g/d_c=2800$ kPa	
	Corner	Sides	Corner	Sides
2D	30.4		47.9	
Circular	30.0		47.2	
$N=1$	31.0		48.2	
$N=4$	23.3	20.5	35.3	31.5
$N=8$	18.1	14.7	27.4	22.4
$N=12$	13.8	11.8	20.9	17.9
$N=16$	11.5	10.1	17.9	15.6
$N=20$	10.1	9.1	16.4	14.0
$N=24$	9.2	8.3	14.4	12.9

759

760

761 Table 5. Normalised maximum hoop force at the encasement, F_g/J_g (%), for different
762 number of columns.

	$J_g/d_c=1120$ kPa		$J_g/d_c=2800$ kPa	
	Corner	Sides	Corner	Sides
2D	1.52		0.96	
Circular	1.50		0.94	
$N=1$	1.55		0.96	
$N=4$	2.33	2.05	1.41	1.26
$N=8$	2.46	2.08	1.55	1.27
$N=12$	2.39	2.04	1.45	1.24
$N=16$	2.30	2.02	1.43	1.25
$N=20$	2.26	2.03	1.47	1.25
$N=24$	2.25	2.03	1.41	1.26

763

764

765 Table 6. Results for different soil material strengths. Reference case.

766

767 (a) Settlement (mm)

	ϕ_s (°)	20	23	26	30
	c_s (kPa)	1	3	6	10
No columns		845.5	291.1	203.9	167.4
2D		291.8	192.4	152.9	135.4
$N=1$		282.7	184.2	143.2	127.8
	$s=1$ m	275.0	182.0	142.2	127.1
$N=4$	$s=2$ m	275.4	181.2	141.3	126.5
	$s=3$ m	265.2	180.8	140.6	125.2
	$s=4$ m	253.3	178.7	139.7	123.2

768

2D: central column

769

770 (b) Maximum hoop force at the encasement (kN/m)

	ϕ_s (°)	20	23	26	30
	c_s (kPa)	1	3	6	10
No columns					
2D		46.2	30.4	24.5	23.3
$N=1$		49.9	31.0	25.2	21.5
	$s=1$ m	26.2	14.8	12.5	11.2
$N=4$	$s=2$ m	23.0	14.7	11.8	10.9
	$s=3$ m	32.4	19.4	14.6	12.9
	$s=4$ m	36.0	24.6	19.9	16.9

771

772 Table 7. Settlement (mm) for different soil layer thicknesses.

	H/B	0.4	0.8	1.2	1.6	2
	H (m)	2	4	6	8	10
No columns		81.0	166.9	236.3	262.6	277.6
2D		47.8	109.3	156.5	181.4	192.4
Circular		45.5	104.3	148.2	171.9	182.6
$N=1$		46.2	106.4	150.7	174.6	184.2
	$s=1$ m	47.5	106.2	148.7	172.7	182.0
$N=4$	$s=2$ m	50.0	107.9	150.3	172.3	181.2
	$s=3$ m	52.6	110.0	146.4	172.3	180.8
	$s=4$ m	56.8	110.7	148.4	170.6	178.7

773

774

775 Table 8. Results for different column lengths. Reference case.

776

777

(a) Settlement (mm)

<i>L</i>	2	4	6	8	10
2D	284.0	268.2	238.7	205.6	192.4
Circular	266.5	254.5	225.6	191.6	182.6
<i>N=1</i>	270.3	256.7	226.6	192.2	184.2
<i>N=4</i>	260.5	229.0	196.9	181.8	179.3
<i>N=8</i>	254.6	216.8	185.8	179.1	177.0
<i>N=12</i>	256.4	218.3	186.5	179.3	177.1
<i>N=16</i>	241.2	205.9	180.0	173.7	176.7

778

Columns on the sides

779

780

781

(b) Maximum hoop force at the encasement (kN/m)

<i>L</i>	2	4	6	8	10
2D	3.3	7.1	19.4	27.1	29.2
Circular	2.4	7.6	19.5	26.2	30.0
<i>N=1</i>	2.5	8.2	20.4	27.6	31.0
<i>N=4</i>	14.8	22.0	21.0	20.4	20.5
<i>N=8</i>	14.2	16.0	14.9	14.6	14.7
<i>N=12</i>	12.3	13.5	12.0	11.8	11.8
<i>N=16</i>	8.7	11.0	9.9	9.6	10.1

782

Columns on the sides

783

784

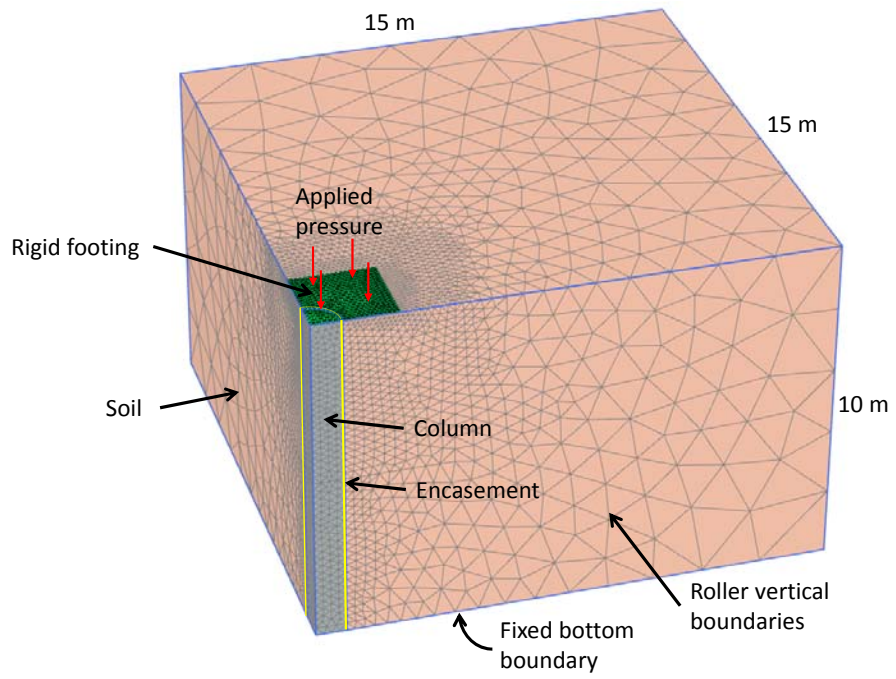
785

786 Table 9. Settlement (mm) for different area replacement ratios.

		$L=2B$		$L=B$	
		$a_r=20\%$	$a_r=30\%$	$a_r=20\%$	$a_r=30\%$
2D					
Circular		112.1	86.4	214.8	191.7
$N=1$		112.4	86.7	214.5	189.8
$N=4$	$s=2$ m	117.2	86.1	184.6	158.6
	$s=3$ m	111.3	86.7	167.3	143.3

787

788



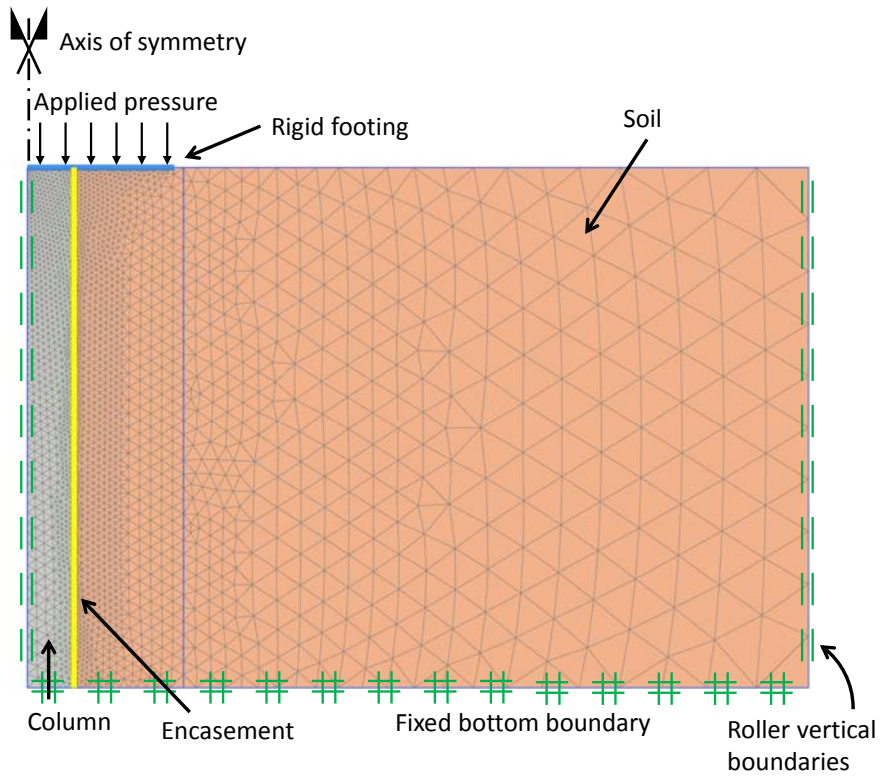
789

790

791

792

Figure 1. 3D finite element model. Reference case.

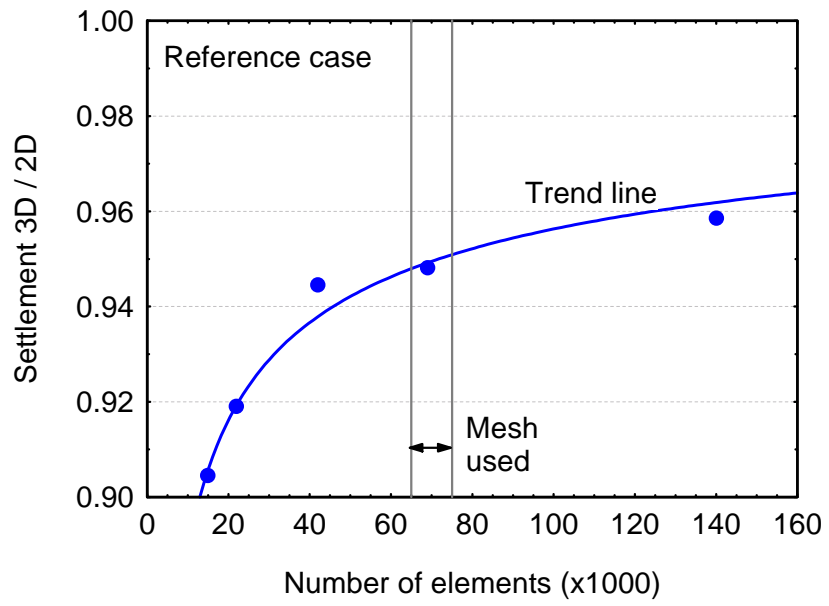


793

794

Figure 2. 2D finite element model. Reference case. Circular footing.

795

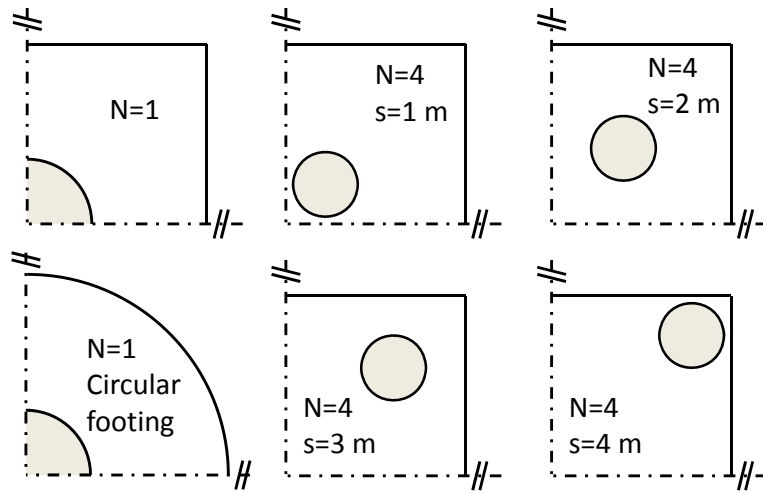


796

797

798

Figure 3. Mesh sensitivity analyses.



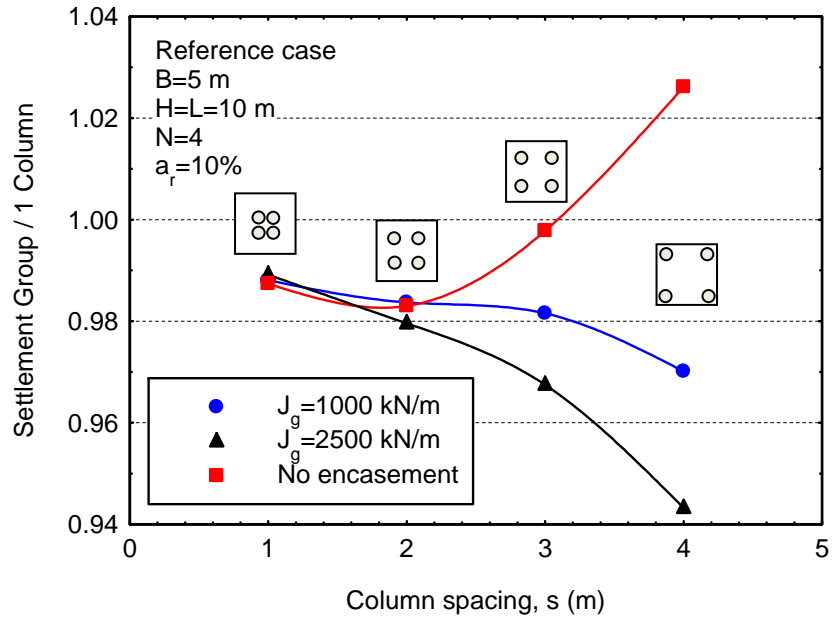
799

800

Figure 4. Groups of encased stone columns for different column positions.

801

802

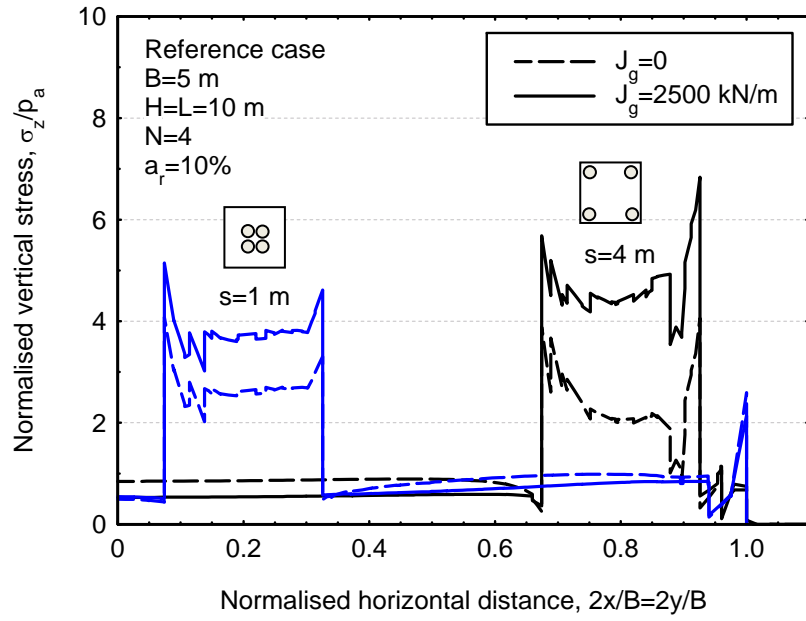


803

804

Figure 5. Influence of column position.

805

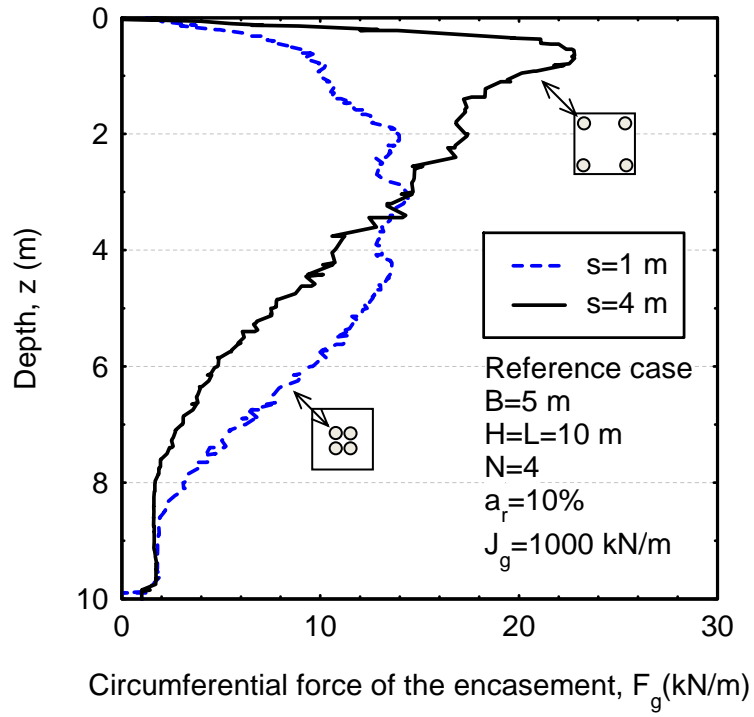


806

807

Figure 6. Vertical stresses beneath the footing. Diagonal section.

808



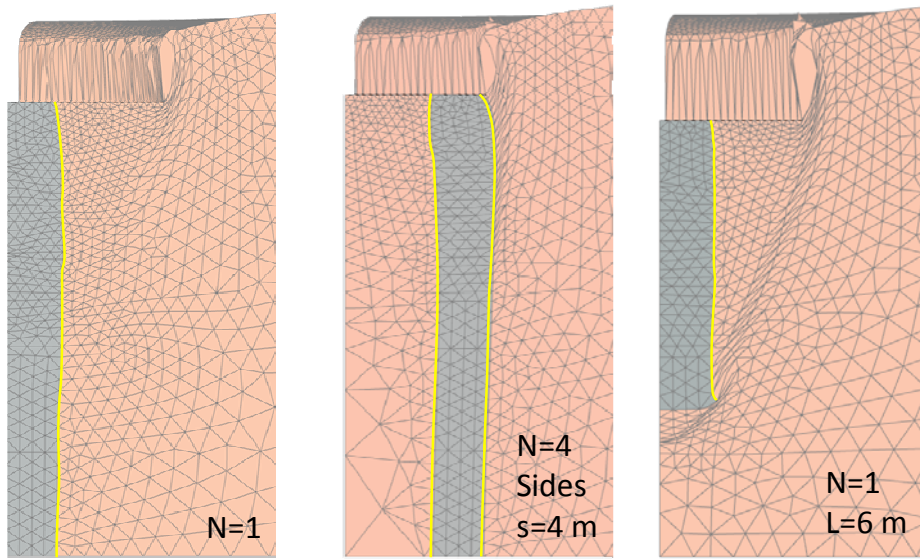
809

810

Figure 7. Circumferential tensile force of the encasement for different column spacings.

811

812



813

814

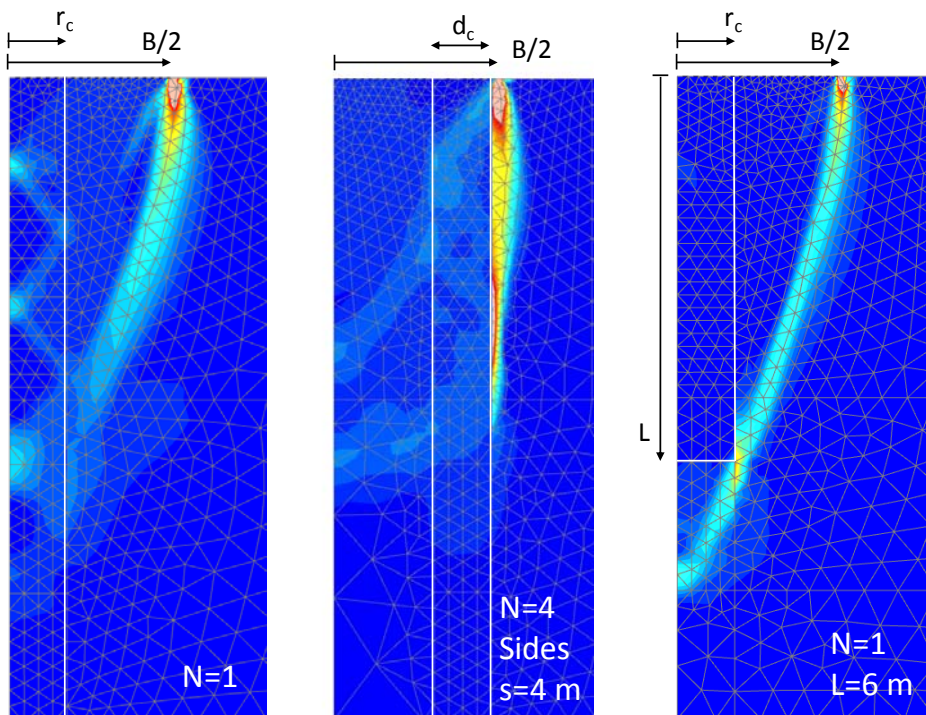
(a)

(b)

(c)

815 Figure 8. Deformation modes: (a) Bulging; (b) Shearing; (c) Punching. Deformed mesh (amplified 10

816 times). Cross section.

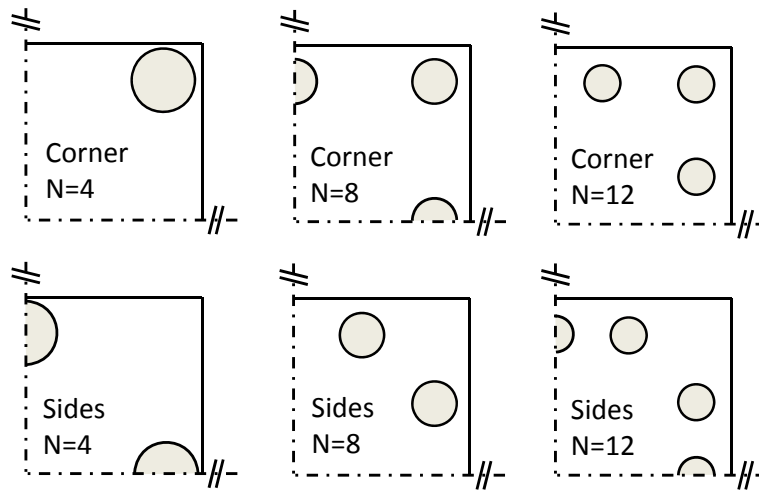


817

818 Figure 9. Incremental shear strains. Blue (dark) lowest value (0) and red highest value (2%). Cross

819 section.

820

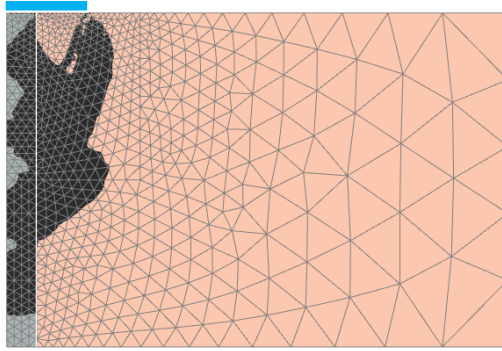


821

822

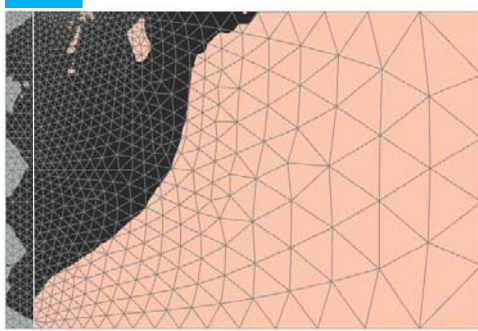
Figure 10. Groups of encased stone columns for different number of columns.

823



(a)

824
825
826

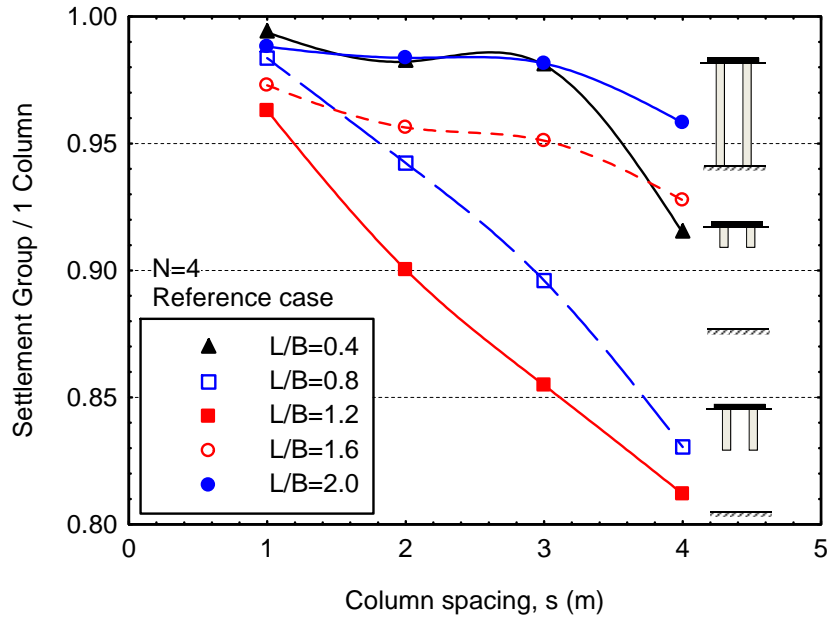


(b)

827
828

829 Figure 11. Zones at failure: (a) $\phi_s=23^\circ$ and $c_s=3$ kPa; (b) $\phi_s=20^\circ$ and $c_s=1$ kPa. Black area: relative shear
830 stress between 99 and 100% of failure.

831



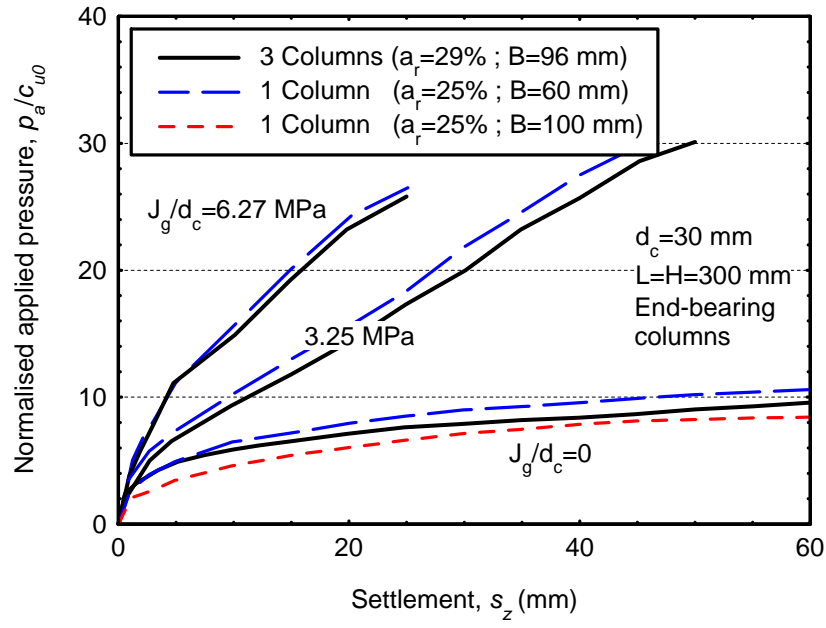
832

833

Figure 12. Influence of column length for different column positions.

834

835

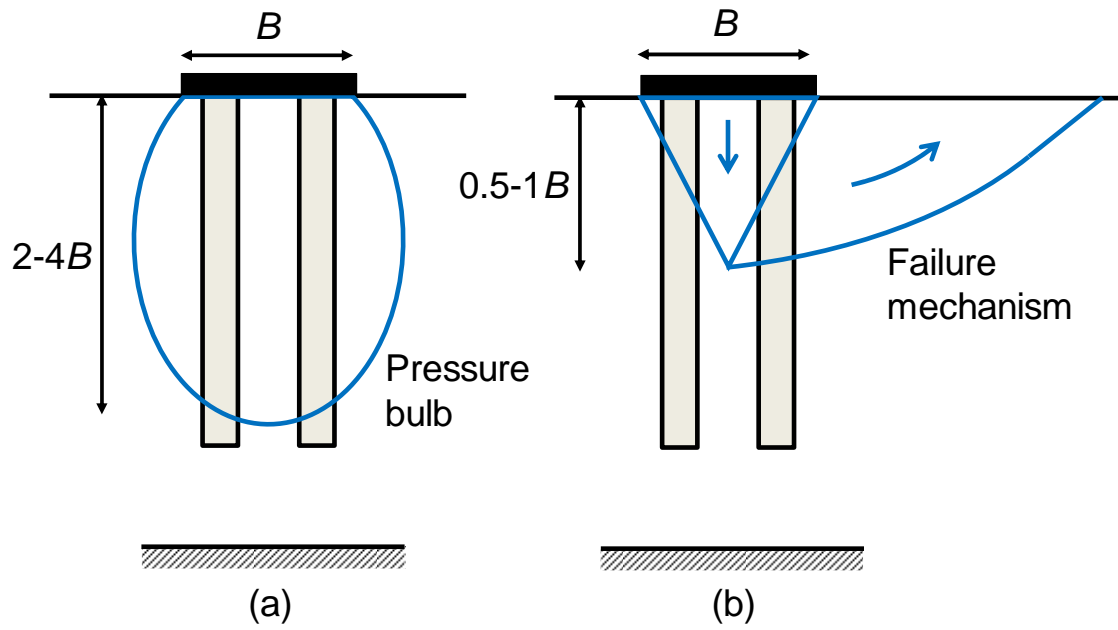


836

837 Figure 13. Comparison between small-group and single column. Laboratory tests (Data taken from Ali et
 838 al., 2014).

839

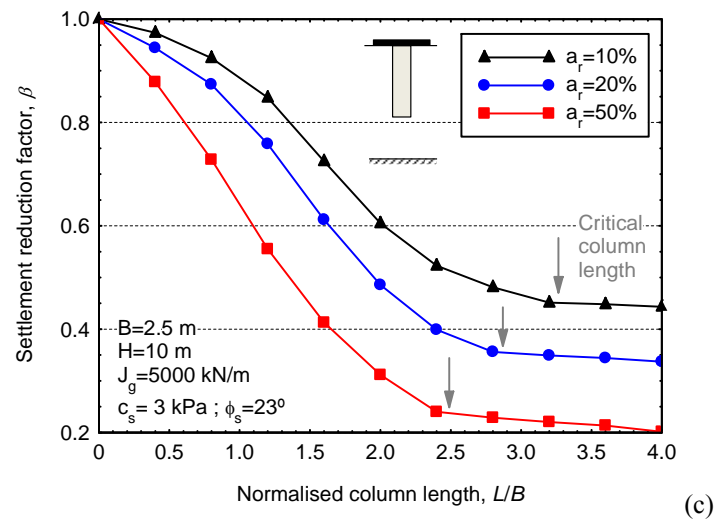
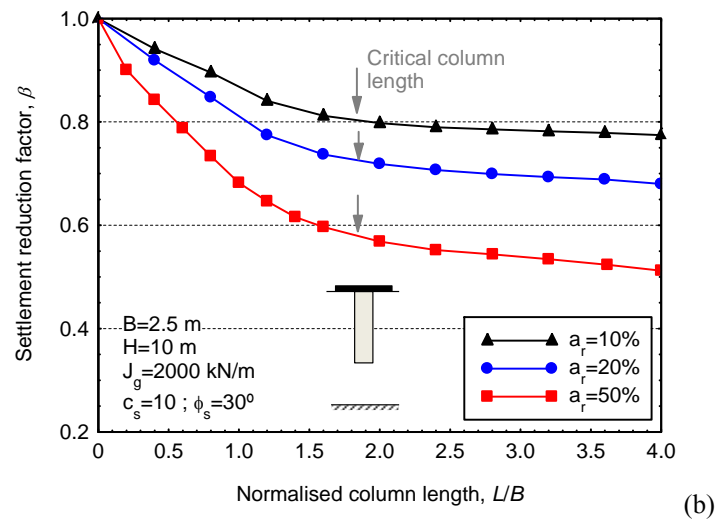
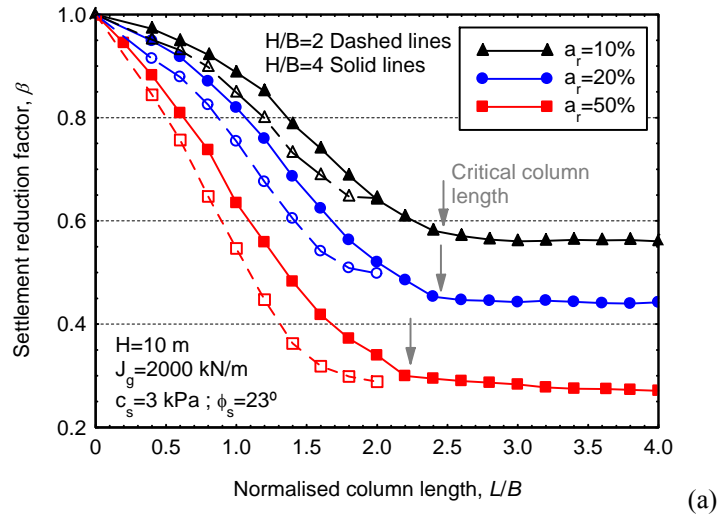
840



841

842 Figure 14. Conceptual justification of critical column length in a homogeneous soil layer: (a) for
 843 settlement reduction; (b) for bearing capacity.

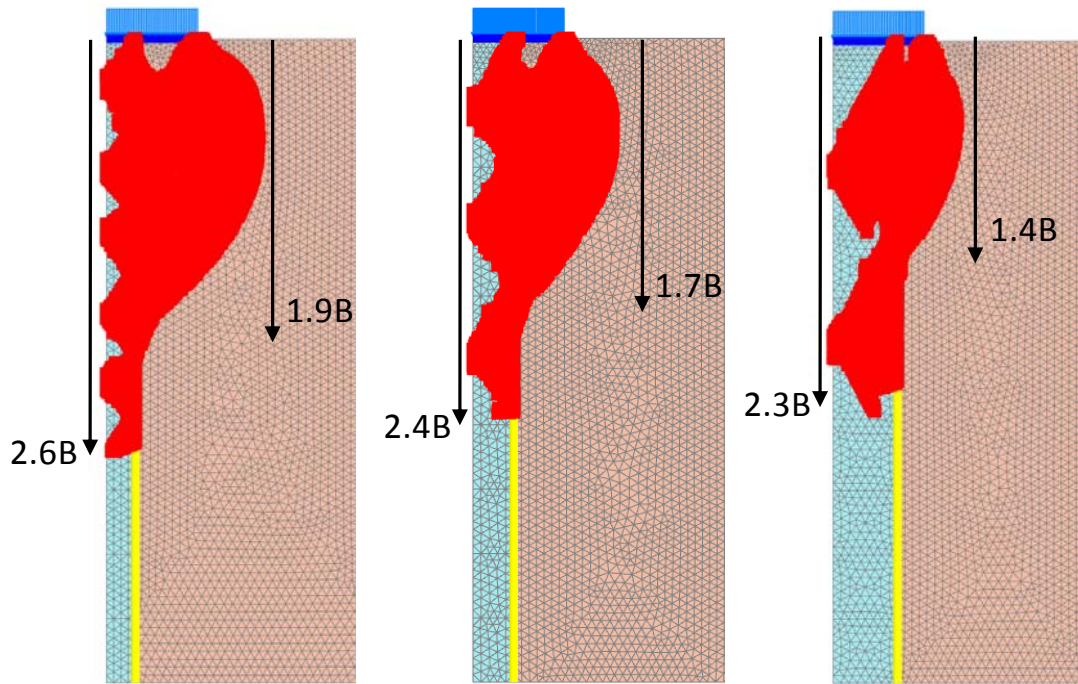
844



848 Figure 15. Critical column length for different area replacement ratios and encasement and soil properties.

849 1 Column (2D) and $B=2.5$ m: (a) Reference case; (b) $c_s=3$ kPa and $\phi_s=30^\circ$; (c) $J_g=5000$ kN/m.

850



851

852

(a)

(b)

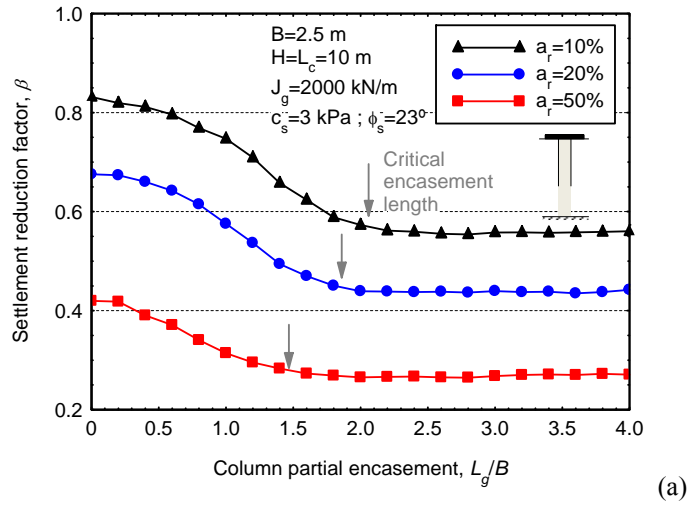
(c)

853 Figure 16. Plastic points (in red). Reference case. 1 Column (2D) and $B=2.5$ m: (a) $a_r=10\%$; (b) $a_r=20\%$;

854 (c) $a_r=50\%$.

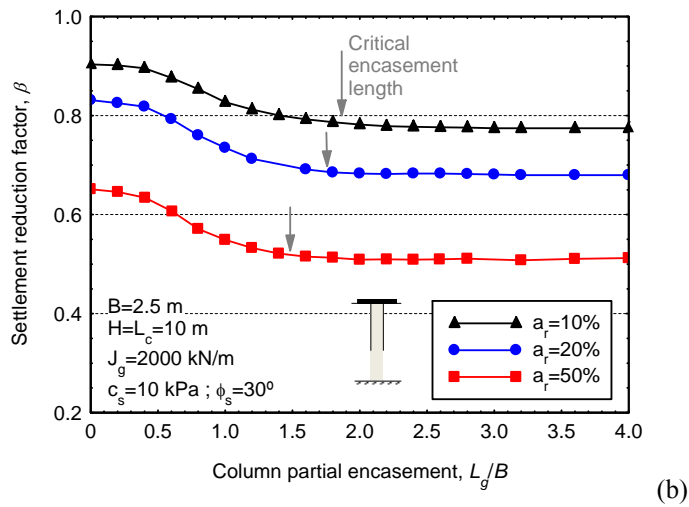
855

856



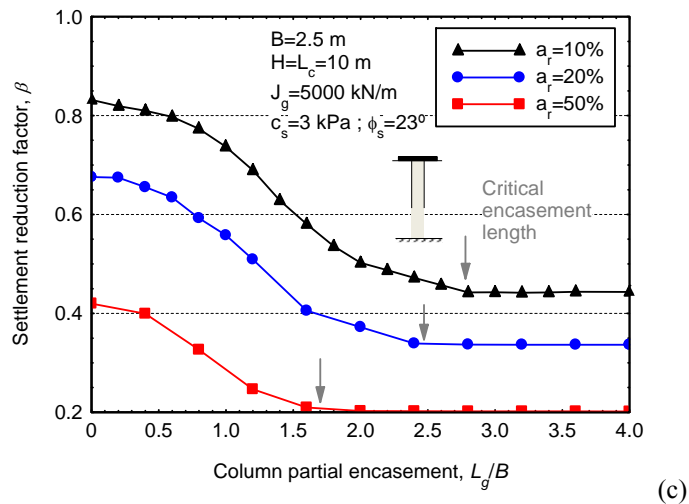
(a)

857



(b)

858



(c)

859 Figure 17. Critical partial encasement length for different area replacement ratios and encasement and soil
 860 properties. 1 Column (2D) and $B=2.5$ m: (a) Reference case; (b) $c_s=3$ kPa and $\phi_s=30^\circ$; (c) $J_g=5000$ kN/m.